TIME SERIES ANALYSIS AND GEOLOGIC MODELING OF RADAR REFLECTORS WITHIN POLAR OUTLIER ICE DEPOSITS IN KOROLEV AND BURROUGHS CRATERS ON MARS. R. A. McGlasson[1], A. M. Bramson[1], M.M. Sori[1], D. E. Lalich[2]. [1]Purdue University Department of Earth, Atmospheric, and Planetary Science, [2]Cornell Center for Astrophysics and Planetary Science. (Corresponding author: rmcglass@purdue.edu).

Introduction: Orbital radar sounding has produced great insights into the shallow Martian subsurface, including extensive mapping of the north and south polar layered deposits (NPLD and SPLD). The PLDs were built up throughout Mars' Amazonian period as layers of water ice with variable dust content were emplaced at the poles. However, the PLDs are not the only exciting polar ice deposits on Mars. Craters near the NPLD and SPLD host ice deposits (the "outlier deposits") [1–2], some of which may have been deposited concurrently with their corresponding PLD [3–4], and others may hold a climate record that is not seen in either PLD [4–5]. A quantitative comparison of the radar reflectors within these deposits is critical for understanding the complete history of polar ice deposition on Mars. We are using two such tools for this task: dynamic time warping (DTW) and a combination of geological and ground penetrating radar (GPR) modeling.

Two prime outlier deposits for this work are the deposits in Korolev crater and Burroughs crater. Korolev crater (72.7°N, 164.5°E) contains an outlier deposit near the NPLD that has been proposed to contain the same pattern of subsurface radar reflectors as the NPLD, and therefore may record the same depositional history as the NPLD [3]. Burroughs crater (72.3°S, 116.6°E) is located near the SPLD, and its deposit has visible layers exposed at the surface and radar reflectors present throughout the vertical extent of the deposit. While radar observations show similar subsurface characteristics as the SPLD (radar reflectors, presence of radar "fog") [4], it is likely that the entirety of the Burroughs ice deposit was emplaced after most of the SPLD was already formed [5]. Using HiRISE imagery of exposed layers at the surface of Burroughs, [5] was able to relate the periodicity of the layer deposition to changes in Mars' orbital characteristics, and suggest that Burroughs, like the PLDs, is strongly controlled by orbital variations.

Although radar observations are lower spatial resolution than HiRISE images, radar observations have a significant advantage for use in paleoclimate studies because they extend throughout the entire depth (and therefore history) of the deposit, rather than being limited to the few hundred meters of visible layers exposed at the surface. Here, we build on previous studies of the outlier deposits in Korolev and Burroughs craters by using new techniques (DTW and Geologic + GPR modeling) to characterize and decipher their radar stratigraphy in order to understand the environmental context of the deposits' formation.

Dynamic Time Warping of the Korolev Deposit: We apply the DTW algorithm to the radar stratigraphy of the NPLD and the Korolev deposit. DTW is a signal-tuning algorithm that can assess the similarity of two signals, even if the relationship between the two may be nonlinear. This method has been successfully used on other paleoclimate records of Earth [6] and Mars [7–9], although they had not previously been tested on radar observations of Martian ice. This technique allows us to quantitatively test the similarity of the radar stratigraphy in the outlying ice deposit in Korolev to that of the NPLD. We use 34 locations across the NPLD and 4 locations from the outlying ice deposit in Korolev crater in our test.

Dynamic Time Warping Results: We first use DTW to tune profiles from all of the Korolev sites to each other in order to see if any one profile can be representative of the whole deposit, which we found to be true for site 4 (K4). We then tune each NPLD profile to K4 to see if any part, or all, of the NPLD had the same stratigraphic pattern as Korolev. We assess the similarity of each tuning by comparing the cross correlation of K4 and the tuned NPLD profile with cross correlation values of K4 and the tunings of 1000 random

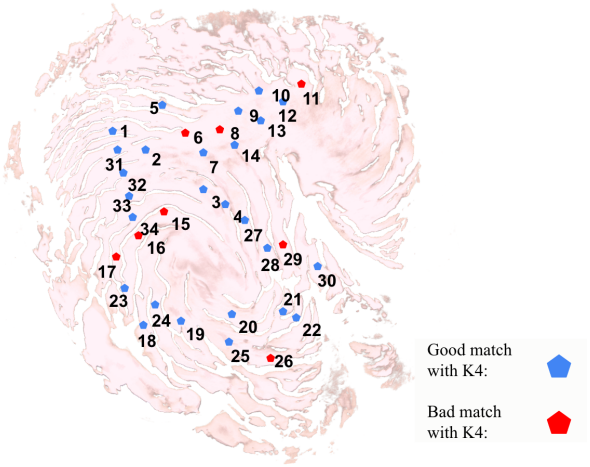

Figure 1. Summary of DTW results showing the depth profile sites across the NPLD, with blue indicating the 26 locations that produced a good match with the representative Korolev site via DTW and red showing the 8 locations that did not.

synthetic profiles (which had the same best-fit skewed gaussian line, mean, standard deviation, and lag-1 autocorrelation as the real signal). We consider a tuning to produce a good match if the cross correlation of the real profiles is better than 95% of the cross correlations with the synthetic profiles. We find that tuning NPLD radar stratigraphy with a representative Korolev site (4) produces a good match via DTW for 26 of 34 NPLD sites (Figure 1). We interpret this result to indicate that the two ice deposits are stratigraphically similar, and may record the same depositional history.

Geological and GPR Modeling of the Burroughs Deposit: Attempts have been made across Martian ice deposits to reconcile the layers that are visible in images with the subsurface interior layering that is represented by the radar reflectors [10,11], however none so far have succeeded in finding a unique solution. Here, we embark upon another attempt at finding a relationship between these observations through a combination of geological modeling with the British Geological Society (BGS) Groundhog software and GPR wave propagation modeling using gprMax. This combination of techniques has been used by [12] to predict RIMFAX radar observations across the Jezero Crater floor. Another objective of our effort is to assess which radar frequencies of current and/or future Martian radar missions would be most useful in reconciling these two types (visible and radar-based) of layered stratigraphies.

Preliminary Geological Modeling Results: We have performed preliminary subsurface geological mapping of the major layers in Burroughs crater (Figure 2) using the software BGS Groundhog [13]. In Groundhog, we used HiRISE imagery and digital terrain models from the edge of the ice deposit in Burroughs crater to identify exposed layers at the surface of the deposit. We identified layers based on visual characteristics (brightness, roughness) and their "stair-stepped" appearance in elevation profiles from HiRISE Digital Terrain Models (DTMs). This stair-stepped appearance arises from variability in the layer's resistance to erosion [7] primarily due to compositional differences. This model will form the input for our GPR modeling.

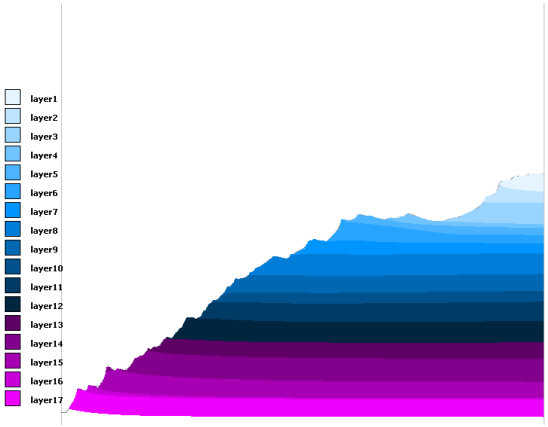

Figure 2. Preliminary subsurface geological model constructed from HiRISE digital terrain model DTEPC_058362_1070_057650_1070_A01, shown with 15× vertical scale.

Future Work: We will take our geological model of the Burroughs deposit and use it as our input subsurface layer geometry for GPR modeling in gprMax, which is a software that solves Maxwell's equations in three dimensions using a finite difference time domain (FDTD) algorithm. We will assign a dust content for each layer based on HiRISE brightness [15], which will allow us to assume a dielectric constant. Using the dust contents inferred from HiRISE brightness, we will run FDTD simulations in gprMax of the constructed subsurface stratigraphy to produce a synthetic radargram. In these simulations we will also test multiple radar frequencies in order to assess what frequencies (if any) would be most able to uniquely relate visible layering and radar reflectors. If/when a DTM is available for the exposed layers at Korolev Crater, we will also apply this technique to Korolev and compare results across the two outlier deposits (one in the north and one in the south).

References: [1] Conway, S. J. et al. (2012). *Icarus*, 220(1), 174–193. [2] Sori, M. M. et al. (2019). *JGR: Planets*, 1–21. [3] Brothers, T. C., and Holt, J. W. (2016). *Geophys. Res. Let.* 42. [4] McGlasson, R. A. et al. (2021). *2021 AGU Fall Meeting*, P32D-05. [5] Sori, M. M. et al. (2022). *Geophys. Res. Let.*, 49. [6] Ajayi, S. et al. (2020). *Geochemistry, Geophysics, Geosystems*, 21(3). [7] Becerra, P. et al. (2016). *JGR: Planets*, 121(8), 1445–1471. [8] Becerra, P. et al. (2019). *Geophys. Res. Let.,* 46(13), 7268–7277. [9] Sori, M. M., et al. (2014). *Icarus*, 235, 136–146. [10] Fishbaugh, K. E. et al. (2010). *Geophys. Res. Let.*, 37(7), 1–5. [11] Lalich, D. E. et al. (2019). *JGR: Planets*, 124(7), 1690–1703. [12] Eide, S., et al. (2021). *IEEE J. Sel. Top. Appl. Earth Obs. Remote Sens.*, 14, 2484–2493. [13] BGS Groundhog Desktop GSIS 2.5.0 (2021). [14] Warren, C. et al. (2016). *Comp. Phys. Comm.*, 209, 163-170. [15] Khuller, A. et al. (2021). *JGR: Planets,* 126(9), e2021JE006910.